RSC Advances

PAPER

View Article Online
View Journal | View Issue

Check for updates

Cite this: *RSC Adv.*, 2017, **7**, 20422

Autonomous self-healing multiwalled carbon nanotube nanocomposites with piezoresistive effect

Tongfei Wu and Biqiong Chen *

Received 10th December 2016
Accepted 3rd April 2017

DOI: 10.1039/c6ra28010b

rsc.li/rsc-advances

Autonomous self-healing fatty acid rubber nanocomposites reinforced by multiwalled carbon nanotubes (MWCNTs) were synthesized by solution blending. The dispersion of MWCNTs in the self-healing fatty acid rubber matrix was observed by scanning electron microscopy. The reinforcement of MWCNTs on the mechanical properties and the self-healing capability of the self-healing fatty acid rubber/MWCNT nanocomposites were investigated by tensile testing. The effect of MWCNT concentration on the electrical conductivity of self-healing fatty acid rubber was studied and the electrically conductive behaviors of self-healing fatty acid rubber/MWCNT nanocomposites were interpreted using the percolation theory and tunneling model. The piezoresistive effect was observed in the nanocomposite with 19.7 vol% MWCNTs, which demonstrates potential for pressure sensing applications.

Open Access Article. Published on 07 April 2017. Downloaded on 4/26/2026 7:23:40 AM.
This article is licensed under a Creative Commons Attribution 3.0 Unported Licence.

Introduction

Inspired by nature, self-healing chemistry is attracting significant interest in the field of electronics.[1] The capability to reconstruct the functionality after rupture will offer a significant advancement towards fabricating safer, longer-lasting and novel electronics. Technically, the recovery of functionalities can either be fully autonomous, or requires external assistance such as heat, light or chemicals to initiate the recovery process.[2] There have been several approaches explored towards building autonomous self-repairing electronics, such as capsule-releasing techniques,[3,4] self-healing rubber/conducting filler hybrids,[5–9] and conducting polymer doughs.[10] In comparison with capsule-releasing techniques, where self-healing cannot take place after capsules are exhausted, the electronics based on self-healing rubbers and polymer doughs both demonstrate that self-healing can act multiple times, providing repeatable recovery of the functionality. Owing to the lack of resilience in polymer doughs, self-healing rubbers are more desirable for flexible/stretchable electronics. The self-healing capability in self-healing rubbers relies on the reversible dynamic bonds of which the association or dissociation can occur spontaneously at ambient conditions, allowing the repair of damages at the molecular level to restore the properties of the original materials.[11] A number of dynamic reversible bonds have been studied, including hydrogen bond,[12–14] metal–ligand interaction,[15] π–π stacking,[16] molecular interdiffusion,[17] and boron/oxygen dative bond.[18]

Self-healing fatty acid rubber is a type of viscoelastic supramolecular polymers made from fatty acids, diethylenetriamine (DETA) and urea, first reported by Leibler and coworkers.[14] The dynamically cross-linked supramolecular network is formed of a large number of di-/tri-functional building blocks with various strongly hydrogen-bonding amide groups. The glass transition temperature (T_g) of this kind of material is generally lower than room temperature (typically 10–25 °C),[19] allowing the association or dissociation of hydrogen bonds to occur spontaneously at ambient conditions and leading to autonomous self-healing behaviors.[19] Owing to the excellent property of self-healing fatty acid rubber, it has stimulated increasing attempts in fabricating self-healing electronics such as high-energy lithium-ion batteries,[20,21] thermal sensors,[8] supercapacitors,[22] and electronic skins.[5,9]

Carbon nanotubes (CNTs) have been explored as a promising nanofiller for conducting polymer nanocomposites, due to their high electrical conductivity (~106 S m^{-1}, metallic type), outstanding mechanical properties (1.5–4.8 GPa in strength), high flexibility, low density, and large aspect ratio (300–1000).[23–26] Theoretically, the large aspect ratio of CNTs enables significant enhancements of electrically conducting properties occurring with a very low percolation threshold for the formation of conducting networks.[27,28] It has been found that the electrical percolation threshold in CNT nanocomposites varies between 0.001 vol% and 1 vol%, depending on the nature of CNTs and polymer used, the dispersion of CNTs in polymer matrix, as well as the fabrication process (*e.g.*, solution blending, melt blending, or *in situ* polymerization).[23,29] Previous studies suggest that the tunneling resistance plays a dominant role in the electrical conductivity of polymer/CNT nanocomposites.[30] And the tunneling resistance is responsive to

Department of Materials Science and Engineering, University of Sheffield, Mappin Street, Sheffield S1 3JD, UK. E-mail: biqiong.chen@sheffield.ac.uk

This journal is © The Royal Society of Chemistry 2017

Open Access Article. Published on 07 April 2017. Downloaded on 4/26/2026 7:23:40 AM. This article is licensed under a Creative Commons Attribution 3.0 Unported Licence.

various external factors. Numerous sensors based on tunneling resistances have been developed utilizing polymer/CNT nanocomposites, including strain sensors,[31] infrared sensors,[32] gas sensors,[33] humidity sensor,[34] and corrosion sensors.[35]

In this work, we prepared self-healing fatty acid rubber/MWCNT nanocomposites with piezoresistive effect by solution blending for pressure sensing applications. The dispersion of MWCNTs in the matrix was observed using a scanning electron microscope. The effects of MWCNTs on mechanical properties and self-healing performance of self-healing fatty acid rubber were examined in depth by tensile tests. Electrically conducting behaviors of self-healing fatty acid rubber/MWCNT nanocomposites were studied using the percolation theory and tunneling model. The piezoresistivity and pressure sensing performance of a selected nanocomposite were investigated.

Experimental

Materials

Pripol 1017 produced from vegetable oils (75–80 wt% dimer acids, 18–22 wt% trimer acids and 1–3 wt% monoacids)[2,19] was provided by Croda International Plc. Multiwalled carbon nanotubes (outer diameter: 10–15 nm, inner diameter: 2–6 nm and length: 0.1–10 μm), diethylenetriamine (DETA, 99%), urea (>99.0%), isopropanol (≥99.7%) and chloroform (≥99.0%) were purchased from Sigma-Aldrich and used as received.

Preparation of self-healing fatty acid rubber solution

Self-healing fatty acid rubber was synthesized from Pripol 1017, DETA and urea following Leibler's method.[8,14,19] Pripol 1017 (46 g) and DETA (16 g) were mechanically stirred continuously at 160 °C for 24 h under a nitrogen atmosphere. The precursor was then dissolved in chloroform (150 mL), followed by washing with a solvent mixture containing 150 mL water and 35 mL methanol for three times using a separatory funnel to remove small-molecule derivatives. Urea (3.5 g) was added into the washed chloroform solution and chloroform was subsequently removed from the system by distillation with an oil bath at 135 °C. The resulting compound was allowed to react at 135 °C for 3 h and then dissolved in isopropanol (300 mL) at 70 °C under mechanical stirring in a nitrogen atmosphere. The concentration of the final self-healing fatty acid rubber in isopropanol was 21.3 wt%.

Preparation of self-healing fatty acid rubber/MWCNT nanocomposites

Self-healing fatty acid rubber/MWCNT nanocomposites were prepared by solution blending. MWCNTs (2 g) were added into 300 mL isopropanol. A Silverson L5M-A shear mixer was employed for MWCNT exfoliation and debundling. The mixture was stirred at 9500 rpm for 20 min within an ice bath to decelerate the evaporation of isopropanol. The solid content of the resultant MWCNT suspension was measured as 0.583 wt% and used for preparing nanocomposites. A desired amount of MWCNT isopropanol suspension was weighed and mixed with self-healing fatty acid rubber solution under magnetically stirring for 2 h. The resulted mixture was poured into a polytetrafluoroethylene (PTFE) dish and kept in a fume cupboard for 24 h to allow the evaporation of most isopropanol. The residual solvent was removed in vacuum at 60 °C for 24 h. Samples with 0, 0.02, 0.04, 0.08, 0.16, and 0.32 mass fractions of MWCNTs in self-healing fatty acid rubber nanocomposites were prepared by this method. The corresponding nominal volume fractions of MWCNTs were 0, 0.0105, 0.0212, 0.0433, 0.0901 and 0.197, respectively, based on densities of self-healing fatty acid rubber (experimentally measured as 0.905 g cm^{-3}) and MWCTs (1.74 g cm^{-3}).[36]

Characterization

Attenuated total reflectance-Fourier transform infrared (ATR-FTIR) spectroscopy was carried out on a Frontier Optica spectrophotometer (PerkinElmer) in the wavenumber region between 4000 to 600 cm^{-1} with a resolution of 1 cm^{-1}. To extract the MWCNTs from the nanocomposite, the fatty acid rubber in the nanocomposite containing 19.7 vol% MWCNTs was dissolved in isopropanol and the MWCNTs were collected by centrifugation. The dissolving-centrifugation cycles had been repeated three times before the separated MWCNTs were dried for FTIR. The microstructure of MWCNTs and the fracture surface of self-healing fatty acid rubber/MWCNT nanocomposite were investigated by scanning electron microscopy (SEM) (Inspect F, FEI) using a 10 keV acceleration voltage. For cross-sectional SEM imaging, the sample was fractured in liquid nitrogen prior to SEM observations. Tensile tests were carried out at room temperature (25 °C) using a Lloyd universal testing machine (Ametek Inc.) with a 10 N load cell and a 100 mm min^{-1} testing speed. For each sample, five specimens were tested. The electrical properties of the sample were monitored in two-point *via* a benchtop multimeter (Agilent 34401A, Keysight Technologies Inc.). For the conductivity test, a cylindrical sample ($\Phi 10 \times 5$ mm) was used and contacted to the circuit *via* two plate aluminium electrodes. For the piezoresistivity measurement, the resistance of the sample was recorded under various external pressures applied by the Lloyd universal testing machine. Differential scanning calorimetry (DSC) was performed on a Diamond DSC (Perkin-Elmer) at a heating/cooling rate of 10 °C min^{-1} in a nitrogen atmosphere. The second heating was used to determine the glass transition temperature of self-healing fatty acid rubber in different nanocomposites to avoid the effect of heating history.

Results and discussion

Characterization of as-synthesized self-healing fatty acid rubber and its MWCNT nanocomposites

Self-healing fatty acid rubber was synthesized through two steps as shown in Scheme 1a: (i) the condensation between dimer/trimer fatty acids and diethylene triamine (DETA), and subsequently (ii) the transamidation of the resulted oligoamidoamines (the precursor) with urea, leading to the extension of the molecular chains, introducing chemical cross-links and intensifying strongly hydrogen bonding points consisting of amide

Open Access Article. Published on 07 April 2017. Downloaded on 4/26/2026 7:23:40 AM.
This article is licensed under a Creative Commons Attribution 3.0 Unported Licence.

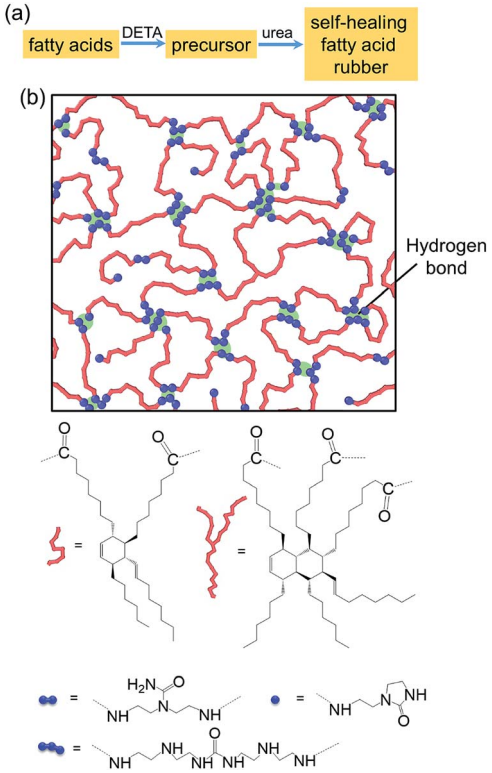

Scheme 1 (a) The synthesis of self-healing fatty acid rubber and (b) its representative chemical structure rich of hydrogen bonds.

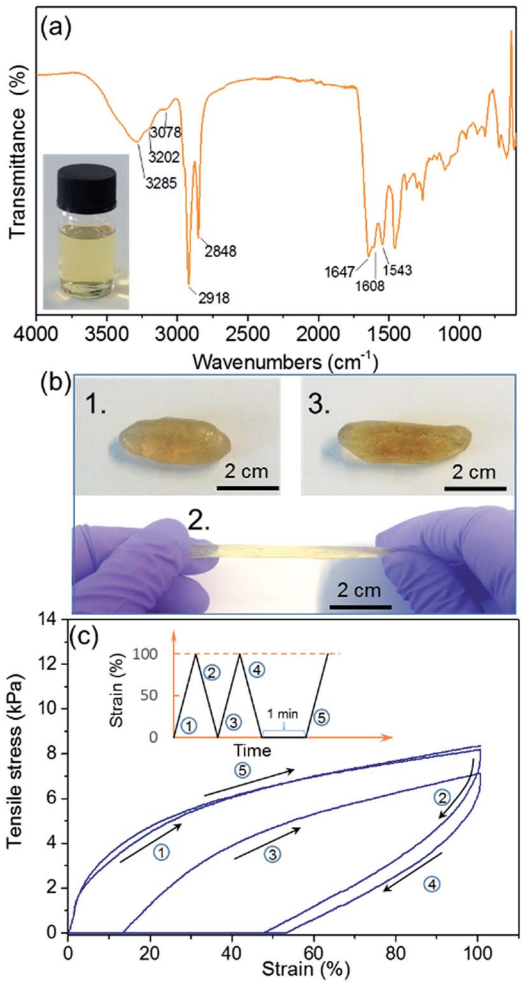

Fig. 1 (a) FTIR spectrum of the as-synthesized self-healing fatty acid rubber product. Inset of (a): photograph of its isopropanol solution. (b) Photographs of the product demonstrating the resilience: (1) original, (2) stretched and (3) released. (c) Cyclic tensile stress–strain curves showing the resilience of the product. Numbers ①–⑤ indicate the sequence of loading and unloading curves as depicted in inset of (c).

groups (Scheme 1b).[14] It was noted that a high density of chemical cross-links would benefit the mechanical properties of products, but reduce their solubility. Therefore, the density of chemical cross-links should be controlled by limiting the reaction time period in the second step to ease the dissolving process. In this work, we chose three hours for the second-step reaction and obtained a clear isopropanol solution (inset of Fig. 1a). The glass transition temperature (T_g) of the product dried from the isopropanol solution was 11.6 °C determined by DSC, which is reliable in comparison with T_g values (typically 10–25 °C) of self-healing fatty acid rubber reported in previous work.[19] The chemical structure was characterized by FTIR in Fig. 1a. The FTIR spectrum shows a number of vibrations: 3285 cm^{-1}, 3202 cm^{-1}, 3078 cm^{-1} and 1543 cm^{-1} (N–H stretching), 2918 cm^{-1} and 2848 cm^{-1} (C–H stretching), 1647 cm^{-1} (C═O stretching in amide), and 1608 cm^{-1} (C═O stretching in urea), which are in excellent agreement with characteristic bands of self-healing fatty acid rubber in the literature.[37] The as-synthesized product appears glassy and resilient, as shown in Fig. 1b. Its autonomous self-healing capability will be discussed below. The deformation hysteresis of the product was measured by cyclic tensile tests (Fig. 1c). Deformation velocity was set to 100 mm min^{-1} and maximum strain was set to 100% of the original length of the sample (the inset of Fig. 1c). The result indicates that the product exhibited a significantly large deformation hysteresis, suggesting a viscoelastic characteristic.[14] The hysteresis energy (*i.e.* the ratio of the area between the first loading and unloading curves (① and ②) to the area under curve ①) was calculated as 75.3%. The residual strain reached 0% (the original point of loading curve ⑤) after 1 min relaxation at stress-free state, suggesting a full recovery in the product after a delayed returning.

To investigate the influence of MWCNTs (Fig. 2a) as an electrically conductive and mechanically reinforcing nanofiller within the self-healing fatty acid rubber, we prepared five self-healing fatty acid rubber/MWCNT nanocomposites with different concentrations of MWCNTs (from 1.05 to 19.7 vol%) by solution blending. Cross-sectional SEM image of the self-healing fatty acid rubber/MWCNT nanocomposite with the highest MWCNT content (19.7 vol%) still demonstrates a homogenous dispersion of MWCNTs in the self-healing fatty acid rubber matrix and a good wettability of self-healing fatty acid rubber on the surface of MWCNTs, as shown in Fig. 2b. This might be related to the nonpolar chemical structure of the fatty acid rubber that contributes to the compatibility, as well as its viscoelastic properties. The interactions between the

This journal is © The Royal Society of Chemistry 2017

Open Access Article. Published on 07 April 2017. Downloaded on 4/26/2026 7:23:40 AM.
This article is licensed under a Creative Commons Attribution 3.0 Unported Licence.

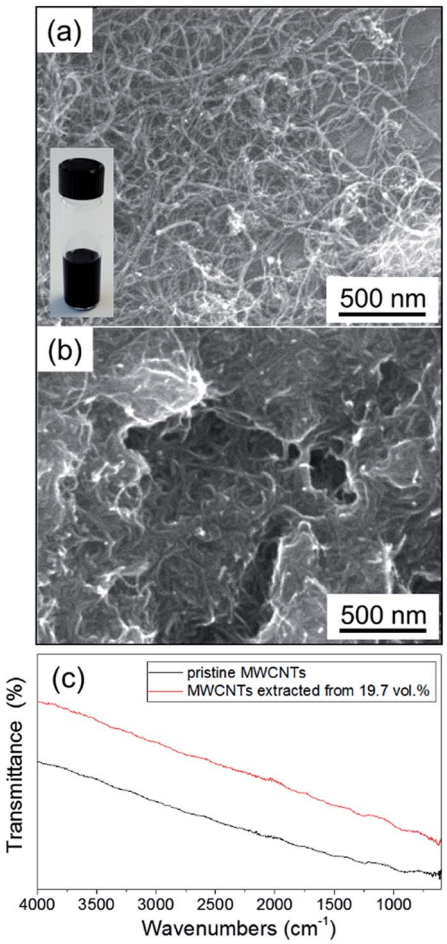

Fig. 2 SEM images of (a) pristine MWCNTs and (b) self-healing fatty acid rubber/MWCNT nanocomposite with 19.7 vol% MWCNTs. Inset of (a): photograph of the MWCNT isopropanol suspension. (c) FTIR spectra of pristine MWCNTs and MWCNTs extracted from the nanocomposite.

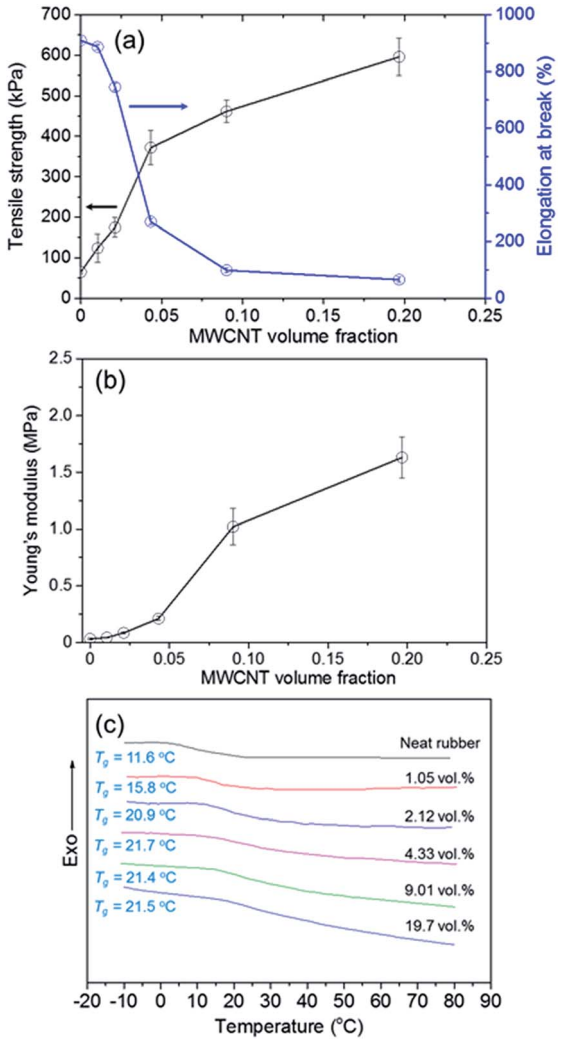

Fig. 3 (a) Tensile strength and elongation at break and (b) Young's modulus of self-healing fatty acid rubber/MWCNT nanocomposites as a function of MWCNT concentration. (c) Glass transition temperature (T_g) of self-healing fatty acid rubber in different nanocomposites measured by DSC during the second heating at a scan rate of 10 °C min^{-1}.

MWCNTs and the fatty acid rubber are physical, as confirmed by FTIR. As shown in Fig. 2c, the MWCNTs separated from the nanocomposite with 19.7 vol% MWCNTs exhibit similar vibration peaks to those of pristine MWCNTs, without the presence of the characteristic absorption peaks of fatty acid rubber.

Mechanical properties of self-healing fatty acid rubber/MWCNT nanocomposites

The reinforcement of MWCNTs on the mechanical properties of self-healing fatty acid rubber was determined by tensile tests. The results are summarized in Fig. 3. The tensile strength, elongation at break, and Young's modulus were 64.8 kPa, 910%, and 35.5 kPa for neat rubber, respectively. The tensile strength increased with MWCNT concentration. The incorporation of MWCNTs raised the tensile strength up to 596 kPa with a MWCNT concentration of 19.7 vol% (corresponding to an 8-time increment), suggesting the efficient stress transfer in the nanocomposite. The elongation at break of self-healing fatty acid rubber/MWCNT nanocomposites decreased dramatically when increasing the concentration of MWCNTs. For instance, the elongation at break was 270% with 4.33 vol% MWCNTs and 65.6% with 19.7 vol% MWCNTs. This can be attributed to the confinement effect of rigid nanofillers on the mobility of polymer chains,[38] which was confirmed by the measurement of T_g of self-healing fatty acid rubber in each nanocomposite (Fig. 3c). It can be seen that T_g has an upward trend with increasing MWCNT concentration, from 11.6 °C for neat rubber up to 21.7 °C with 4.33 vol% MWCNTs. This large T_g shift (~10 °C) suggests the efficient suppression of the mobility of self-healing fatty acid rubber chains by MWCNTs. That is attributable to the large specific surface area of MWCNTs[39] and good wettability of self-healing fatty acid rubber on the surface of MWCNTs. Young's modulus of self-healing fatty acid rubber/MWCNT nanocomposites increased significantly with the content of MWCNTs. The improvement was 5.89 times with 4.33 vol% MWCNTs, 32.6 times with 9.01 vol% MWCNTs, and 52.3 times

Open Access Article. Published on 07 April 2017. Downloaded on 4/26/2026 7:23:40 AM.
This article is licensed under a Creative Commons Attribution 3.0 Unported Licence.

with 19.7 vol% MWCNTs, in comparison with that for neat rubber. These reinforcements are ascribed to the excellent physical and mechanical properties of MWCNTs as well as a good dispersion of MWCNTs in the rubber matrix.[40]

A key feature of self-healing fatty acid rubber is its autonomous, room-temperature (RT, 25 °C) mechanically self-healing property. It means, when self-healing fatty acid rubber suffers cracks or fractures, simply bringing the broken pieces together will lead to spontaneous healing. Fig. 4a demonstrates the mechanically self-healing behavior of the MWCNT-reinforced self-healing fatty acid rubber nanocomposite (19.7 vol%). According to the literature,[5] the mechanical healing efficiency can be calculated as the ratio of the restored toughness (the area under the stress–strain curve) to the original toughness. Fig. 4b compares the typical tensile stress–strain curves of samples healed for 5 min at two different temperatures (RT and 50 °C) and their healing efficiencies are summarized in Fig. 4c. The toughness of neat rubber was able to almost fully recover (99.5%) after 5 min of contact at RT. For self-healing fatty acid rubber/MWCNT nanocomposites, the self-healing capability decreased dramatically with the MWCNT concentration. For instance, the healing efficiency was determined as 43.2% with 1.05 vol% MWCNTs after 5 min of contact at RT and 12.1% with 19.7 vol% MWCNTs. The decreasing self-healing capability with increasing MWCNT amount can be attributed to the fact that MWCNTs could form a rigid network hindering the migration of self-healing fatty acid rubber for the contact through confining polymer chains.[38] Hence, the healing efficiency can be improved by heating, because an elevated temperature facilitates the mobility of polymer chains. In comparison with the performance at RT, the self-healing capability at 50 °C was improved to 89.7%, 89.1%, 88.5%, 71.2% and 46.8% for the self-healing fatty acid rubber/MWCNT nanocomposite with 1.05, 2.12, 4.33, 9.01 and 19.7 vol% MWCNTs, respectively.

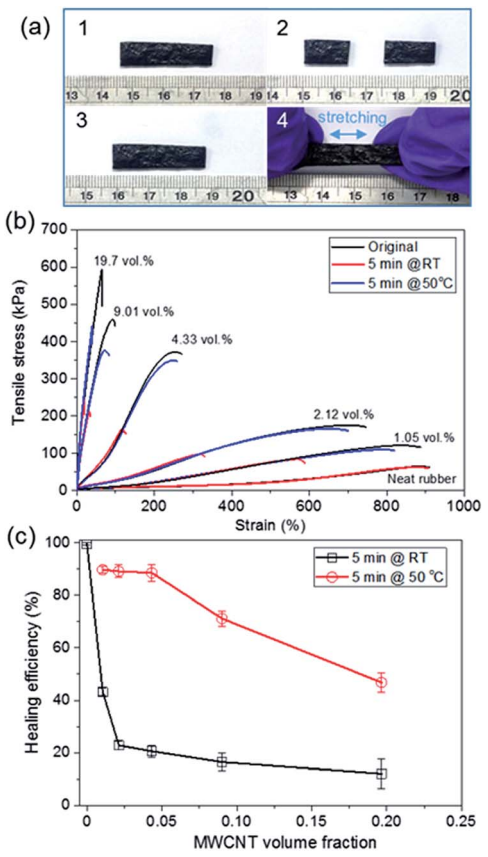

Fig. 4 (a) Photographs of the self-healing fatty acid rubber/MWCNT nanocomposite with 19.7 vol% MWCNTs demonstrating the autonomous healing property at room temperature (RT, 25 °C): (1) original; (2) completely severed; (3) contacted for healing; and (4) healed after 5 min of contact. (b) Typical tensile stress–strain curves of original samples and samples healed for 5 min at RT and 50 °C. (c) Self-healing efficiency of samples at two different temperatures.

Electrically conducting behaviors of self-healing fatty acid rubber/MWCNT nanocomposites

The MWCNT network provides a continuous conducting network in the insulating rubber matrix. The experimentally determined electrical conductivity (σ) increases with the MWCNT concentration, from 1.53×10^{-5} S cm^{-1} with 1.05 vol% MWCNTs to 5.01×10^{-3} S cm^{-1} with 19.7 vol% MWCNTs (Fig. 5a). The conductivity data were interpreted by the percolation theory and tunneling model.[41,42] In classical percolation theory, the dependence of σ values of the composites on the conductive filler concentration (p) above the percolation threshold (p_c) can be described by a scaling law as shown in eqn (1).[43]

$$\sigma = \sigma_0(p - p_c)^t \text{ for } p > p_c \quad (1)$$

here σ_0 is a fitted conductive constant and t is the critical exponent. A non-linear curve fitting of the experimental data was performed in order to obtain the best fitted values of constants in eqn (1). t was determined as 1.67, in fair agreement with the value of 1.6–2.0 obtained by Monte Carlo studies in three dimensions.[44] The value of p_c was 4.53×10^{-3} (*i.e.* 0.453 vol%) and 0.084 S cm^{-1} for σ_0. The value of σ_0 should approach the conductivity of the MWCNT cluster itself (typically 1–5 S cm^{-1} under 0.1–5 MPa as reported in the literature[45]). However, the fitted σ_0 was much lower than those values. This might be caused by the presence of the contact resistance between the clusters of MWCNTs in the nanocomposites, which was formed by the thin insulating rubber layer on MWCNTs and significantly reduced the effective conductivity of the MWCNT network.[46] That means the electrons needed more energy to tunnel from one conductive cluster to another separated by the thin insulating layer.

According to the thermal fluctuation-induced tunneling model,[47] the electrical conductivity for a homogeneous conductive filler/insulating polymer composite can be described by the behavior of a single tunnel junction at a given temperature, and a linear relation between ln σ and $p^{-1/3}$ is expected, namely ln $\sigma \propto p^{-1/3}$. From the inset of Fig. 5a, it can be seen that the electrical conduction in self-healing fatty acid rubber/MWCNT nanocomposites followed well the tunneling model. Therefore, the low value of σ_0 suggests a good wettability of self-healing fatty acid rubber on the surface of MWCNTs, which is in accordance with

 This journal is © The Royal Society of Chemistry 2017

Open Access Article. Published on 07 April 2017. Downloaded on 4/26/2026 7:23:40 AM.
This article is licensed under a Creative Commons Attribution 3.0 Unported Licence.

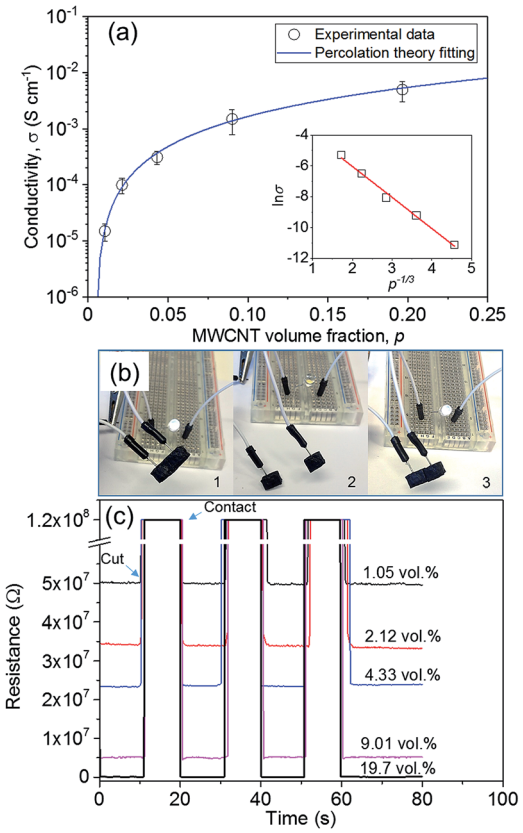

Fig. 5 (a) Electrical conductivity of self-healing fatty acid rubber/MWCNT nanocomposites *versus* the MWCNT concentration. Inset of (a): plot of $\ln\sigma$ *vs.* $p^{-1/3}$. (b) Demonstration of the self-repairing property of the self-healing fatty acid rubber/MWCNT nanocomposite (19.7 vol%) in an LED circuit: (1) original; (2) completely severed; (3) healed by applying a gentle force (~1 kPa) for ~1 s. (c) Resistance *versus* time during the electrically healing process.

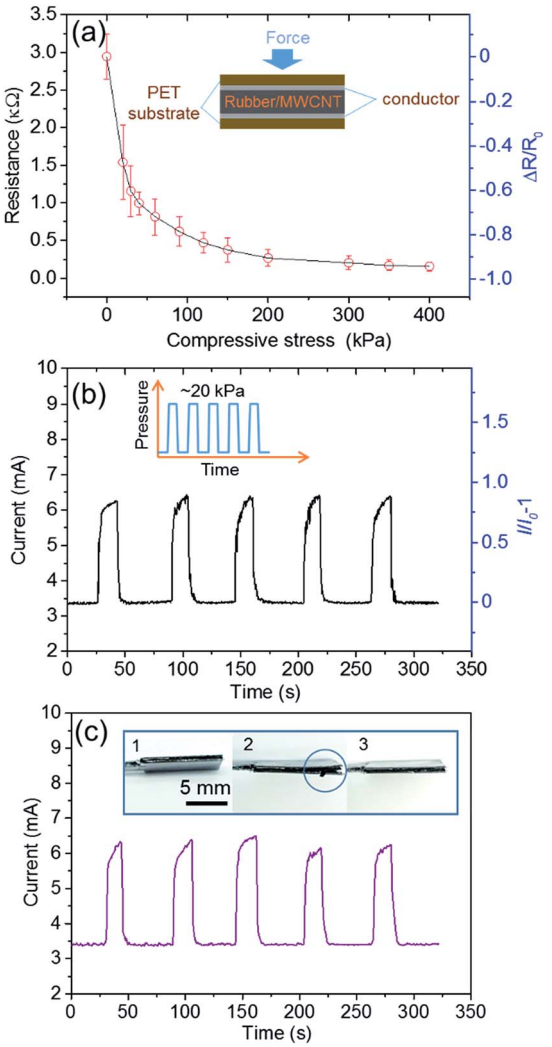

Fig. 6 (a) Resistance (R) *versus* pressure for the self-healing fatty acid rubber/MWCNT nanocomposite with 19.7 vol% MWCNTs. The inset of (b) is the schematic setup for the pressure-responsive test. (b) Current (I) *versus* time for the as-established device in response to pulse pressure application of approximately 20 kPa. The dynamic test was conducted at a bias voltage of 10 V. Inset of (b): applied pressure against time. (c) Current *versus* time for the healed device after a damage demonstrated in the inset of (c): (1) original; (2) with a cut in the middle of rubber/MWCNT layer; (3) healed by applying a press (~400 kPa) for ~10 s.

the observation of SEM. Fig. 5b demonstrates the self-repairing behavior of an electronic circuit containing the self-healing nanocomposite. The change in resistance during the repeated self-healing processes is shown in Fig. 5c. It can be seen that the resistance immediately dropped to nearly its original value, as soon as the two fracture surfaces were gently brought together. The conductive healing efficiency is determined as the ratio of the original resistance to the restored resistance. The healing efficiency is calculated as higher than 98.2% for all self-healing fatty acid rubber/MWCNT nanocomposites.

Based on the tunneling model, the compression-induced reduction in the thickness of insulating polymer layer would raise the electrical conductivity, leading to the piezoresistive effect.[48] The piezoresistive effect in self-healing fatty acid rubber/MWCNT nanocomposite with 19.7 vol% MWCNTs was investigated (Fig. 6a). The device setup with a sandwich configuration was shown in the inset of Fig. 6a. In the device, the middle nanocomposite layer (rubber/MWCNT) with a thickness of 100 μm was formed by compression and self-adhered to the two Al conductors. As anticipated, the resistance decreased with increasing pressure, but exhibited a non-linear relation in the range from zero pressure up to 400 kPa. For instance, the resistance (R_0) was 2.94×10^3 Ω at zero pressure, 618 Ω at 90 kPa, 268 Ω at 200 kPa, and 158 Ω at 400 kPa, where the corresponding reduction factors ($\Delta R/R_0$) were −79.0%, −90.9% and −94.6%, respectively. Dynamic pressure sensitivity was monitored while measuring the current variations with the repeated application of ~20 kPa (Fig. 6b). Under a compression of ~20 kPa, the measured current becomes noticeably higher (a sensitivity ($\Delta I/I_0 - 1$) of 90%); once the force was released, the current gradually decreased in 7–10 s to the initial value. These dynamic compression characteristics are comparable or superior to those of devices based on CNT/polyurethane composites and CNT/vinyl ester composites.[49,50] With these fast response and recovery times, the as-established

Open Access Article. Published on 07 April 2017. Downloaded on 4/26/2026 7:23:40 AM. This article is licensed under a Creative Commons Attribution 3.0 Unported Licence.

pressure sensor exhibited a significant change in the intensity of current signal. The five testing cycles showing the same profiles suggested good repeatability in responses to dynamic loading. Fig. 6c demonstrates that the as-established sensor could be repaired by applying a press (~400 kPa) for ~10 s after a damage (like a cutting) in the rubber/MWCNT layer, owning to the self-healing capability of rubber/MWCNT nanocomposites.

Conclusions

Autonomous self-healing conducting nanocomposites were synthesized by embedding MWCNTs in the self-healing matrix of fatty acid rubber. The tensile strength and Young's modulus of the self-healing fatty acid rubber were significantly improved by the addition of MWCNTs. However, the elongation at break was dramatically reduced, owing to the confinement effect of rigid nanofillers on the mobility of polymer chains. The nanocomposites demonstrated repetitive rapid mechanically self-healing capability at ambient temperature where the healing efficiency could be further improved through increasing the mobility of polymer chains by heating. The electrically conducting behaviors of the nanocomposites followed the percolation theory and tunneling model. The nanocomposite with 19.7 vol% MWCNTs exhibited a non-linear piezoresistive effect. In dynamic pressure sensing test, the nanocomposite exhibited a fast recovery time (7–10 s) and good repeatability, while a sensitivity of 90% was achieved at ~20 kPa. The sensor made up of the nanocomposite could be repaired by applying a press after a damage, owning to its self-healing capability.

Acknowledgements

This project is supported by the European Commission's Horizon 2020 research and innovation programme under the Marie Skłodowska-Curie grant agreement No. 656467.

Notes and references

1 S. J. Benight, C. Wang, J. B. H. Tok and Z. Bao, *Prog. Polym. Sci.*, 2013, **38**, 1961–1977.
2 B. J. Blaiszik, S. L. B. Kramer, S. C. Olugebefola, J. S. Moore, N. R. Sottos and S. R. White, *Annu. Rev. Mater. Res.*, 2010, **40**, 179–211.
3 E. Palleau, S. Reece, S. C. Desai, M. E. Smith and M. D. Dickey, *Adv. Mater.*, 2013, **25**, 1589–1592.
4 B. J. Blaiszik, S. L. B. Kramer, M. E. Grady, D. A. McIlroy, J. S. Moore, N. R. Sottos and S. R. White, *Adv. Mater.*, 2012, **24**, 398–401.
5 B. C. K. Tee, C. Wang, R. Allen and Z. Bao, *Nat. Nanotechnol.*, 2012, **7**, 825–832.
6 H. Sun, X. You, Y. Jiang, G. Guan, X. Fang, J. Deng, P. Chen, Y. Luo and H. Peng, *Angew. Chem., Int. Ed.*, 2014, **53**, 9526–9531.
7 S. Michel, B. T. T. Chu, S. Grimm, F. A. Nuesch, A. Borgschulte and D. M. Opris, *J. Mater. Chem.*, 2012, **22**, 20736–20741.
8 Y. He, S. Liao, H. Jia, Y. Cao, Z. Wang and Y. Wang, *Adv. Mater.*, 2015, **27**, 4622–4627.
9 E. D'Elia, S. Barg, N. Ni, V. G. Rocha and E. Saiz, *Adv. Mater.*, 2015, **27**, 4788–4794.
10 J. Y. Oh, S. Kim, H. K. Baik and U. Jeong, *Adv. Mater.*, 2016, **28**, 4455–4461.
11 M. W. Keller, S. R. White and N. R. Sottos, *Adv. Funct. Mater.*, 2007, **17**, 2399–2404.
12 J. Hentschel, A. M. Kushner, J. Ziller and Z. Guan, *Angew. Chem., Int. Ed.*, 2012, **51**, 10561–10565.
13 Y. Chen, A. M. Kushner, G. A. Williams and Z. Guan, *Nat. Chem.*, 2012, **4**, 467–472.
14 P. Cordier, F. Tournilhac, C. Soulie-Ziakovic and L. Leibler, *Nature*, 2008, **451**, 977–980.
15 D. Mozhdehi, S. Ayala, O. R. Cromwell and Z. Guan, *J. Am. Chem. Soc.*, 2014, **136**, 16128–16131.
16 S. Burattini, B. W. Greenland, D. H. Merino, W. Weng, J. Seppala, H. M. Colquhoun, W. Hayes, M. E. Mackay, I. W. Hamley and S. J. Rowan, *J. Am. Chem. Soc.*, 2010, **132**, 12051–12058.
17 M. A. Rahman, L. Sartore, F. Bignotti and L. Di Landro, *ACS Appl. Mater. Interfaces*, 2013, **5**, 1494–1502.
18 A. Juhász, P. Tasnádi and L. Fábry, *Phys. Educ.*, 1984, **19**, 302.
19 D. Montarnal, F. Tournilhac, M. Hidalgo, J. L. Couturier and L. Leibler, *J. Am. Chem. Soc.*, 2009, **131**, 7966–7967.
20 C. Wang, H. Wu, Z. Chen, M. T. McDowell, Y. Cui and Z. Bao, *Nat. Chem.*, 2013, **5**, 1042–1048.
21 Y. Zhao, Y. Zhang, H. Sun, X. Dong, J. Cao, L. Wang, Y. Xu, J. Ren, Y. Hwang, I. H. Son, X. Huang, Y. Wang and H. Peng, *Angew. Chem., Int. Ed.*, 2016, **55**, 14384–14388.
22 H. Wang, B. Zhu, W. Jiang, Y. Yang, W. R. Leow, H. Wang and X. Chen, *Adv. Mater.*, 2014, **26**, 3638–3643.
23 M. Moniruzzaman and K. I. Winey, *Macromolecules*, 2006, **39**, 5194–5205.
24 N. G. Sahoo, S. Rana, J. W. Cho, L. Li and S. H. Chan, *Prog. Polym. Sci.*, 2010, **35**, 837–867.
25 R. H. Baughman, A. A. Zakhidov and W. A. de Heer, *Science*, 2002, **297**, 787–792.
26 J. N. Coleman, U. Khan and Y. K. Gun'ko, *Adv. Mater.*, 2006, **18**, 689–706.
27 Y. Wang, G. J. Weng, S. A. Meguid and A. M. Hamouda, *J. Appl. Phys.*, 2014, **115**, 193706.
28 C. Li and T. W. Chou, *Appl. Phys. Lett.*, 2007, **90**, 174108.
29 W. Bauhofer and J. Z. Kovacs, *Compos. Sci. Technol.*, 2009, **69**, 1486–1498.
30 C. Li, E. T. Thostenson and T. W. Chou, *Appl. Phys. Lett.*, 2007, **91**, 223114.
31 N. Hu, Y. Karube, C. Yan, Z. Masuda and H. Fukunaga, *Acta Mater.*, 2008, **56**, 2929–2936.
32 B. Pradhan, K. Setyowati, H. Liu, D. H. Waldeck and J. Chen, *Nano Lett.*, 2008, **8**, 1142–1146.
33 K. H. An, S. Y. Jeong, H. R. Hwang and Y. H. Lee, *Adv. Mater.*, 2004, **16**, 1005–1009.
34 K. P. Yoo, L. T. Lim, N. K. Min, M. J. Lee, C. J. Lee and C. W. Park, *Sens. Actuators, B*, 2010, **145**, 120–125.

 This journal is © The Royal Society of Chemistry 2017

Open Access Article. Published on 07 April 2017. Downloaded on 4/26/2026 7:23:40 AM.
This article is licensed under a Creative Commons Attribution 3.0 Unported Licence.

35 J. L. Kenneth, K. Junhee, P. L. Jerome, K. Nadine Wong Shi and A. K. Nicholas, *Smart Mater. Struct.*, 2007, **16**, 429.
36 S. H. Kim, G. W. Mulholland and M. R. Zachariah, *Carbon*, 2009, **47**, 1297–1302.
37 D. Montarnal, P. Cordier, C. Soulié-Ziakovic, F. Tournilhac and L. Leibler, *J. Polym. Sci., Part A: Polym. Chem.*, 2008, **46**, 7925–7936.
38 P. Rittigstein, R. D. Priestley, L. J. Broadbelt and J. M. Torkelson, *Nat. Mater.*, 2007, **6**, 278–282.
39 J. H. Lehman, M. Terrones, E. Mansfield, K. E. Hurst and V. Meunier, *Carbon*, 2011, **49**, 2581–2602.
40 H. Xia and M. Song, *Soft Matter*, 2005, **1**, 386–394.
41 D. Stauffer, *Introduction to the percolation theory*, Francis and Taylor, London, 2nd edn, 1991.
42 P. Sheng, E. K. Sichel and J. I. Gittleman, *Phys. Rev. Lett.*, 1978, **40**, 1197–1200.
43 M. Weber and M. R. Kamal, *Polym. Compos.*, 1997, **18**, 711–725.
44 M. T. Connor, S. Roy, T. A. Ezquerra and F. J. Baltá Calleja, *Phys. Rev. B: Condens. Matter Mater. Phys.*, 1998, **57**, 2286–2294.
45 B. Marinho, M. Ghislandi, E. Tkalya, C. E. Koning and G. de With, *Powder Technol.*, 2012, **221**, 351–358.
46 Z. Ounaies, C. Park, K. E. Wise, E. J. Siochi and J. S. Harrison, *Compos. Sci. Technol.*, 2003, **63**, 1637–1646.
47 T. A. Ezquerra, M. Kulescza and F. J. Baltá-Calleja, *Synth. Met.*, 1991, **41**, 915–920.
48 L. Chen, G. H. Chen and L. Lu, *Adv. Funct. Mater.*, 2007, **17**, 898–904.
49 J. J. Ku-Herrera and F. Avilés, *Carbon*, 2012, **50**, 2592–2598.
50 T. Zhai, D. Li, G. Fei and H. Xia, *Composites, Part A*, 2015, **72**, 108–114.